

Collateral Constraints and Asset Composition*

Chengzi Yi

European University Institute

April 10, 2025

Abstract

This paper studies how collateral constraints shape firms' asset composition between real estate and non-real-estate capital. I build a dynamic two-asset model with convex and non-convex adjustment costs and asset-specific pledgeability, and I structurally estimate it using data on Chinese listed manufacturing firms. The estimates indicate substantially higher fixed costs of adjusting real estate and greater pledgeability of real estate. With these frictions, the model matches the observed right-skewed distribution of the real-estate-to-non-real-estate ratio and the declining real-estate share with firm size. Removing financial frictions eliminates precautionary investments and reduces aggregate capital and revenue; removing both financial frictions and fixed costs raises both. In both counterfactuals, aggregate TFPR increases. In a real estate crisis scenario in which real estate becomes non-pledgeable, investment tilts towards non-real estate and aggregate capital rises due to the higher collateral value of non-real estate; however, misallocation worsens: aggregate TFPR falls by 3.6% and revenue by 0.3%.

*I am grateful to my advisers, Russell Cooper and Alexander Monge-Naranjo, for their guidance and support. This work was partly conducted while visiting Universitat Pompeu Fabra, and I thank Andrea Caggese for his hospitality and advice. I would also like to thank Isaac Baley, Jesús Bueren, Basile Grassi, Guanliang Hu, Priit Jeenas, Winfried Koeniger, Ernest Liu, Umberto Muratori, Lukas Nord, Yaxuan Qi, Gianmarco Ruzzier, Jonathan Willis, and Piotr Żoch, as well as seminar and conference participants, for helpful comments and discussions. Any remaining errors are my own. Email: Chengzi.Yi@eui.eu

1 Introduction

Firms allocate investment across different types of capital, including non-real-estate assets, such as equipment and machinery, and real estate assets, such as industrial structures and commercial properties. These categories of capital differ significantly in their specificity, divisibility, and liquidity. Adjustment of these capital goods incurs varying costs, influencing firms' investment portfolio decisions. In a frictional economy with collateral constraints, these goods also differ in pledgeability, adding another layer of complexity to investment dynamics. This paper shows that, for Chinese manufacturing firms, real estate assets have higher pledgeability, but their adjustments incur higher fixed costs than for non-real-estate assets.

Studying firms' investment allocation in real estate capital becomes especially relevant in the context of the recent real estate crisis in China. The crisis, epitomised by the 2021 collapse of Evergrande, one of the country's largest property developers, highlights systemic vulnerabilities in the Chinese real estate market. The sharp decline in real estate prices, coupled with restrictive real estate policies, can limit firms' ability to pledge real estate assets for financing. This dynamic is particularly concerning for non-real-estate firms that rely on real estate collateral to fund investments. Characterising Chinese firms' capital investment decisions sheds light on the extent to which real estate pledgeability influences broader capital allocation and aggregate economic outcomes.

The asset composition of Chinese listed manufacturing firms shows two salient features. First, the ratio of real estate to non-real-estate assets (RE/Non-RE) is highly right-skewed across firms. Second, firms with smaller total capital allocate a larger share of capital to real estate than larger firms.

I model firms' capital adjustment across two types of capital, which are combined using a CES aggregator in production. Investment dynamics and asset composition are jointly determined by the elasticity of substitution, adjustment costs, and collateral constraints. Adjustments to both assets involve convex and non-convex costs. Investment (including adjustment costs) is financed with internal funds and external borrowing, with the latter constrained by collateral limits. Both convex adjustment costs and collateral constraints smooth the capital accumulation process, whereas non-convex costs lead to lumpy adjustments. Collateral constraints affect the investment trade-off in two ways: first, a constraint that binds today increases the benefit of disinvestment; second, a potentially binding future constraint makes collateral more valuable, increasing the benefit of investment. Consequently, firms' asset composition may adjust in anticipation of future constraints, driven by differences in the pledgeability of real estate and non-real-estate assets, a mechanism also emphasised by Perez-Orive (2016).

I estimate the decreasing-returns-to-scale revenue function, the CES aggregator, and idiosyncratic profitability shocks using the generalised method of moments, with moment conditions derived from the quasi-differenced revenue function. The estimates suggest that the two types of capital inputs are perfect complements in production. This implies that, in a frictionless

economy, there is an optimal asset composition, and the ratio of real estate to non-real-estate assets remains constant. However, this contradicts the observed skewed distribution of the RE/Non-RE ratio across firms. Intuitively, introducing adjustment and financial frictions helps explain this non-degenerate distribution.

I then estimate the adjustment-cost and pledgeability parameters for both assets using the simulated method of moments, targeting moments of investment dynamics and capital composition. The two assets differ in two key respects. First, the fixed costs of adjusting real estate, which average 24% of flow revenue when investing, are significantly higher than for non-real estate. Second, real estate is more pledgeable than non-real estate: one unit of non-real estate can secure external financing equivalent to 2.328 units of non-real estate, whereas the corresponding figure for real estate is 2.547.

To disentangle the effects of adjustment frictions and financial frictions, I compare four model variants: (i) without collateral constraints; (ii) without external financing; (iii) with collateral constraints and symmetric pledgeability; and (iv) with collateral constraints and asymmetric pledgeability. In model (i), high fixed costs of investing in real estate generate variation in asset composition across firms and help explain the decline in the share of real estate in capital as firm size increases. With high fixed costs for real estate investment, firms often remain inactive in their real estate holdings while adjusting non-real-estate assets in response to profitability shocks, leading to variation in composition. Smaller firms hold more real estate despite the high fixed costs, as the marginal return on capital is higher under decreasing returns to scale. This mechanism operates only when financial constraints are sufficiently loose. In model (ii), when external funding is unavailable and constraints are therefore extremely tight, investment in both asset types is suppressed, particularly in real estate due to the high fixed costs, resulting in much less variation in asset composition.

Moreover, the introduction of collateral constraints and asymmetry in pledgeability in model (iv) allow the model to better match salient features of Chinese firms' asset composition compared to the other specifications. Financial constraints are occasionally binding and are more likely to bind for smaller firms, whose marginal return on capital is higher and whose access to external funding is more limited. With asymmetric pledgeability, firms tilt investment towards more pledgeable assets due to a precautionary saving motive. The combination of asymmetric non-convex costs and asymmetric pledgeability helps generate the observed negative correlation between capital size and the share of real estate in total capital, thereby favouring model (iv).

Using this estimated model, I run counterfactuals that progressively remove fixed adjustment costs and collateral constraints. As frictions in the economy decrease, asset composition moves closer to the optimum implied by the production technology. The average RE/Non-RE ratio falls by 16% when financial constraints are removed and by 28% when both financial constraints and fixed adjustment costs are removed. The allocation across firms improves in both scenarios, as aggregate TFPR increases. In the absence of financial frictions, profitable firms can grow larger, and aggregate TFPR rises by 5%. By contrast, when fixed adjustment

costs are also removed, aggregate TFPR increases by only 3%. High fixed costs act as a selection mechanism, allowing only sufficiently profitable firms to grow larger. Removing these frictions has different effects on aggregate capital and revenue. Without financial frictions, the collateral value of capital falls to zero, eliminating the precautionary incentive to invest. Therefore, aggregate capital decreases by 4%, and aggregate revenue correspondingly decreases by 0.8%. If fixed costs are also removed, aggregate capital increases by 36.7% and aggregate revenue by 31.8%.

I then analyse a scenario in which real estate becomes entirely non-pledgeable. In a real estate crisis, real estate prices often decline and become more volatile. Lower prices directly reduce the value of collateral, limiting its use for securing financing. Under the incentive compatibility condition, the pledgeable value of collateral is determined by its lowest possible price realisation; greater volatility therefore further diminishes the attractiveness of real estate as secure collateral. When real estate is non-pledgeable, financial constraints tighten and the collateral value of non-real-estate capital increases. Consequently, aggregate capital rises by 3%, and the average RE/Non-RE ratio decreases by 9%, bringing asset composition closer to the technology-implied optimum. However, despite the increase in aggregate capital and the improved asset composition within firms, the economy experiences greater distortions, as reflected in a 3.6% decline in aggregate TFPR and a 0.3% drop in aggregate revenue.

The remainder of this paper is organised as follows. Section 2 summarises the related literature; Section 3 presents the dynamic model and discusses the mechanism; Section 4 presents the data, and discusses the GMM and SMM estimation procedures and the results. Section 5 presents the counterfactual exercises. Section 6 concludes.

2 Related Literature

This paper highlights the importance of real estate as collateral for financing investments. Chaney et al. (2012) and Gan (2007) demonstrate that real estate assets play a critical role as collateral in the US and Japan, showing that changes in real estate values due to price fluctuations have significant impacts on firms' capital accumulation—a mechanism referred to as the “collateral channel.” Bahaj et al. (2020) provide evidence that firm owners' homes serve as a source of finance. In the context of the Chinese economy, Wu et al. (2015) find no evidence of a collateral channel effect, whereas Chen et al. (2015) document a significant collateral channel effect for private firms. These studies leverage real estate price shocks and exogenous variation in real estate values to examine the effect of collateral value on firm investment.

This paper contributes to the literature by investigating the collateral channel effect in the Chinese market using a structural approach. It provides a framework for re-examining empirical evidence on the role of collateral in China and other markets. The closest related

study is Catherine et al. (2022), which estimates a dynamic investment model with collateral constraints and integrates it into a general equilibrium framework to quantify the aggregate effects of financing constraints. However, their model assumes exogenous and constant real estate holdings across all firms and periods. This paper allows for endogenous decisions on real estate assets and directly addresses the potential endogeneity in real estate investment.

This paper also relates to the literature on financial frictions and investment composition, which examines the implications of financial frictions when firms have heterogeneous investment projects (Matsuyama, 2007; Aghion et al., 2010; Perez-Orive, 2016; Ottonello and Winberry). Theoretical studies show that firms tend to shift towards investment projects that are less subject to financial imperfections when credit constraints tighten. Empirically, Kermani and Ma (2023) provide evidence of heterogeneity in the liquidation values of different types of capital assets. In this paper, I distinguish real estate assets from other capital assets and estimate the production technology, adjustment costs, and pledgeability parameters that jointly explain firms' investment dynamics. The findings reveal heterogeneous pledgeability, which further enables a quantification of the effects of financial frictions on asset composition.

Finally, this paper contributes to the literature on capital adjustment costs, building on work by Abel and Eberly (1994), Abel and Eberly (1999), Doms and Dunne (1998), and Cooper and Haltiwanger (2006), which highlight the role of non-convex adjustment costs and examine the lumpiness in investment dynamics. Midrigan and Xu incorporate both non-convex capital adjustment costs and borrowing frictions into their model to evaluate the extent to which these frictions explain resource misallocation. Yan (2012) estimates a capital adjustment model with non-convex costs for Chinese manufacturing plants by plant ownership type and quantifies the source of misallocation across plant types. As for different types of capital assets, Nilsen and Schiantarelli (2003) distinguishes between equipment and buildings and documents empirical evidence of more inaction and more spikes in investments in buildings. Chiavari and Goraya distinguishes between tangible and intangible assets, and their estimation shows higher costs in adjusting intangible assets. This paper complements these studies by finding a large fixed cost of adjusting real estate capital in a structural model and contributes to understanding the components of convex adjustment costs for different types of assets.

3 Capital Adjustment Model

Firms' investments in two heterogeneous assets are characterised by an extension of Hayashi (1982). The model is different from Hayashi (1982) mainly in three aspects: firstly, there are two types of capital assets, which are both production inputs; secondly, the adjustments of both assets are subject to heterogeneous convex and non-convex adjustment costs; thirdly, firms' investments are financed through both internal funding and external funding, and the external funding is bounded by collateral constraints.

Firms are subject to idiosyncratic profitability shocks z and determine their investments in non-real-estate capital k and real estate capital h . There is time to build for both assets. The idiosyncratic profitability shock $\log(z)$ follows an AR(1) process, i.e., $\log(z_t) = \rho_z \log(z_{t-1}) + \sigma_z \xi_t$, $\xi_t \sim N(0, 1)$. The revenue function allows for decreasing returns to scale. k and h are bundled by a CES aggregator as equation 1. σ is the elasticity of substitution between k and h . When $\sigma \rightarrow 1$, capital input is a Cobb-Douglas function of k and h , i.e., $(\frac{k}{a})^a (\frac{h}{1-a})^{1-a}$. When $\sigma \rightarrow 0$, capital input is a Leontief function of k and h , i.e., $\min\{\frac{k}{a}, \frac{h}{1-a}\}$. When $\sigma \rightarrow +\infty$, capital is the sum of the two assets, i.e., $k + h$.

$$\pi(k, h, z) = z \left\{ (a^{\frac{1}{\sigma}} k^{\frac{\sigma-1}{\sigma}} + (1-a)^{\frac{1}{\sigma}} h^{\frac{\sigma-1}{\sigma}})^{\frac{\sigma}{\sigma-1}} \right\}^{\alpha}, \quad \alpha \leq 1. \quad (1)$$

$C(k, k')$ and $\tilde{C}(h, h')$ are the cost functions of adjusting k and h , respectively. The cost includes both convex and non-convex components. x_k and x_h denote the investment of k and h , respectively. The purchase price of k is normalised to one. There is plenty of empirical evidence for various forms of adjustment costs. The convex adjustment costs can account for the observed slow and smoothed adjustments of capital, which may arise from the capacity constraints of the capital goods provider or the gradual building/installing process. They may also account for the effect of financial capacities. The nonconvex costs can capture the need for organisational restructuring or worker retraining during the adjustment episode¹.

$$C(k, k') = \begin{cases} x_k + \frac{\gamma}{2} \frac{x_k^2}{k} + F_k k & \text{if } x_k \neq 0; \\ 0 & \text{if } x_k = 0; \end{cases}$$

$$\tilde{C}(h, h') = \begin{cases} p_h x_h + \frac{\omega}{2} \frac{x_h^2}{h} + F_h h & \text{if } x_h \neq 0; \\ 0 & \text{if } x_h = 0; \end{cases}$$

The value function has an extensive margin as equation 2 due to the non-convex adjustment costs.

$$V(k, h, z) = \max\{V^a(k, h, z), V^k(k, h, z), V^h(k, h, z), V^n(k, h, z)\} \quad (2)$$

$V^a(k, h, z)$ is the value if adjusting both assets:

$$V^a(k, h, z) = \max_{k', h' \geq 0} \pi(k, h, z) - C(k, k') - \tilde{C}(h, h') + \beta \mathbb{E}V(k', h', z') \quad (3)$$

$$\text{s.t. } C(k, k') + \tilde{C}(h, h') \leq \pi(k, h, z) + \phi_k k(1 - \delta_k) + \phi_h p_h h(1 - \delta_h)$$

¹The nonconvex costs consist only of scale-dependent fixed costs, but not the irreversibility $p_k^- < 1$ and $p_h^- < 1$. $p_k^- < 1$ and $p_h^- < 1$ are not well identified in the estimation by the negative investment spikes since k has a high depreciation rate according to the data, and F_h tends to be high in the estimation. As a consequence, changing p_k^- and p_h^- introduces little variation to the moments. I thus omit the irreversibility. However, the model can still generate negative investment spikes in the simulation that are close to the observed ones.

$V^k(k, h, z)$ is the value if only adjusting non-real-estate capital:

$$\begin{aligned} V^k(k, h, z) = \max_{k' \geq 0} \quad & \pi(k, h, z) - C(k, k') + \beta \mathbb{E}V(k', h(1 - \delta_h), z') \\ \text{s.t. } & C(k, k') \leq \pi(k, h, z) + \phi_k k(1 - \delta_k) + \phi_h p_h h(1 - \delta_h) \end{aligned} \quad (4)$$

$V^h(k, h, z)$ is the value if only adjusting real estate capital:

$$\begin{aligned} V^h(k, h, z) = \max_{h' \geq 0} \quad & \pi(k, h, z) - \tilde{C}(h, h') + \beta \mathbb{E}V(k(1 - \delta_k), h', z') \\ \text{s.t. } & \tilde{C}(h, h') \leq \pi(k, h, z) + \phi_k k(1 - \delta_k) + \phi_h p_h h(1 - \delta_h) \end{aligned} \quad (5)$$

$V^n(k, h, z)$ is the value of inaction:

$$V^n(k, h, z) = \pi(k, h, z) + \beta \mathbb{E}V(k(1 - \delta_k), h(1 - \delta_h), z') \quad (6)$$

The capital adjustment costs $C(k, k') + \tilde{C}(h, h')$ are financed by firms' revenue π and some external funding. The collateral constraints limit the amount of external funding to no more than the value of collateral $\phi_k(1 - \delta_k)k + \phi_h p_h(1 - \delta_h)h$. The parameters ϕ_k and ϕ_h govern the pledgeability of k and h , respectively. This form of collateral constraint has been commonly used in the literature: it assumes that the debt capacity is limited by a fraction of the assets pledged. The parameter ϕ is usually interpreted as the liquidation value of the capital stock (for instance, Kiyotaki and Moore (1997)). However, as discussed in Kermani and Ma (2023), models of this form of collateral constraints have used a variety of calibrated or estimated values for ϕ , which can range from 15%-20% as in Catherine et al. (2022) to 80% as in Moll (2014) and Midrigan and Xu (2014). Kermani and Ma (2023) estimates the average PPE liquidation recovery rate to be 35% for a sample of U.S. firms.

The model abstracts from the dynamic decision on debt by assuming intratemporal borrowing: Firms can borrow at the beginning of the period, and the amount of debt cannot exceed the collateral value, governed by ϕ_k and ϕ_h . If debt > 0 , firms pay off the debt by raising equity at the end of the period². Firms' investments are financed by their flow profit and within-period liquid debt. The assumption of intratemporal debt can significantly simplify the computation of the model. However, in practice, firms may also finance their investments through cash stock or intertemporal debt, which has been thoroughly studied in Almeida et al. (2004), Bates et al. (2009), and James and Lirely (2022). Omitting the dynamic cash/debt decision may, therefore, bias the estimates of the pledgeability parameters. If firms that anticipate future investment needs accumulate cash in advance and thus rely less on external borrowing, or if the debt can be carried over for more than one period, the financial constraint would be less likely to bind, and the pledgeability parameter estimate would likely be positively biased. On the other hand, firms' decisions on cash holdings can also be orthogonal to capital accumulation if they are driven by a transaction motive, as in Miller and Orr (1968) or a tax motive, as in Foley et al. (2007). To examine the role

²There is no equity issuance cost by assumption.

of cash/debt for Chinese listed manufacturing firms, in the Appendix A.4, I follow Görtz et al. (2023) and show that positive investment spikes are associated with an increase in debt during the adjustment period and one year after, indicating limited debt rollover. Firms do not appear to accumulate cash before the investment spikes.

The introduction of collateral constraints in the dynamic capital adjustment problem can affect firms' investment decisions in the following way: in the extensive margin, the collateral constraints affect the cost of action if they are binding in the current period, but also affect the benefit of action if they are binding in the future. Similarly, other things equal, the binding constraints in the current period increase the benefit of disinvestment or the cost of investment. The binding constraint in the next period increases the benefit of investment or the cost of disinvestment. This is similar to the precautionary saving channel discussed by Perez-Orive (2016).

4 Structural Estimation

4.1 Data and Empirical Patterns

The sample is Chinese publicly listed firms from 2003 to 2019. The Chinese stock market was piloted in 1989, and the accounting data from 1990 to 2019 are collected and published by the CSMAR database³. The price index of capital goods is from the Chinese Statistical Bureau. Only the observations after 2003 are kept because there is no detailed classification of fixed assets before 2003. There has been an increasing number of firms over the years as more firms enter the stock market. I only keep firms with observations of more than three consecutive years and obtain an unbalanced panel with 2,137 firms and 21,783 firm-year observations.

The fixed asset classification is taken from the financial statement appendix (section: fixed assets). The real estate capital includes houses, buildings, and land. The non-real-estate capital includes equipment, machinery, and other facilities. From the appendix, I collect the original value, the accumulated depreciation, and the annual depreciation for the total fixed assets and the real estate assets. The nominal values for non-real-estate assets are the residual from subtracting the real estate value from the total value. The stock values of both capital assets are recovered by the perpetual inventory method using the information on fixed assets from 1990 to 2019. The detailed procedure is described in the Appendix A.1.

The investment rate is the ratio between the amount of deflated net investment and the beginning-of-period capital stock. I exclude the outlier observations in the bottom and top

³The balance sheet, the income statement, and the cash flow statement are taken from FS_Combas, FS_Comins, FS_Comscfi. The classification of the sector and other firm identifiers are from TRD_Co. The addendum to the financial statement(section: fixed assets) is from FN_Fn020.

percentiles to avoid measurement errors that may arise from manually classifying assets. The revenue is defined as the cash flow net of labour cost and before investment expenditure, which is measured by earnings before interest, tax, depreciation, and amortisation (EBITDA) and obtained by adding back the sum of operating tax, financing cost, depreciation, and amortisation to operating profit. I deflate the nominal value with a capital goods price index so that revenue is measured in units of non-real-estate capital.

Table 1 describes the key variables in the sample. The average investment rate of non-real capital is 0.31, and the average investment rate of real estate capital is 0.22. These are higher than the average investment rate in Yan (2012), which uses a sample of above-scale manufacturing firms during 2005-2007. The sample in this paper consists of large listed firms, and the sample period covers the period after the four trillion stimulus, which may explain the difference. I merge the sample of listed firms with the sample of above-scale manufacturing firms. For those firms in both samples, I compare the investment rates calculated from the data of the two samples and find little difference.

Table 1: Descriptive Statistics

	mean	sd	p25	p50	p75	N
inv. rate	0.27	0.49	0.04	0.13	0.32	18,395
inv. rate: k	0.31	0.55	0.05	0.16	0.38	17,218
inv. rate: h	0.22	0.50	0.00	0.07	0.25	17,914
$\log(\pi)$	18.32	1.41	17.40	18.20	19.15	20,144
$\log(k)$	18.83	1.63	17.72	18.70	19.83	19,430
$\log(h)$	18.43	1.46	17.50	18.36	19.24	20,259
h/k	0.80	0.57	0.38	0.65	1.07	18,460

Note: The statistics in this table describe the constructed variables for all the observations in the sample. k denotes the stock value of non-real-estate capital, and h denotes the stock value of real estate capital. π denotes the revenue.

The model incorporates a rich structure of capital adjustment costs for both assets. Figure A1 presents the distribution of investment rates at the firm-year level for Chinese listed firms and demonstrates a fat right tail and asymmetry between positive and negative investments for both types of assets. Moreover, the investment rates, especially those of real estate capital, are centred around zero, i.e., inaction. Figure A2 shows that investments in both assets tend to comove with each other, potentially explained by the complementarity of the two assets in production and/or the aggregate shock. When calculating the targeted data moments in the estimation, the aggregate component in the shock is controlled by removing the year fixed effects.

Figure 1 presents the distribution of the RE/Non-RE ratio across firms for the sample period from 2003 to 2019. Panel (a) shows a heavily skewed distribution, where most firms have a RE/Non-RE ratio smaller than 1, indicating a relatively low proportion of real estate assets

in their capital structure. However, a small proportion of firms exhibit significantly higher RE/Non-RE ratios, contributing to the long right tail of the distribution.

Panel (b) of Figure 1 illustrates the average RE/Non-RE ratio across capital stock quintile groups. The data reveal a clear declining trend: firms in the lowest quintile of total capital stock hold the highest average RE/Non-RE ratio, while firms in the top quintile exhibit the lowest average ratio. This suggests that smaller firms allocate a greater share of their capital to real estate assets compared to larger firms.

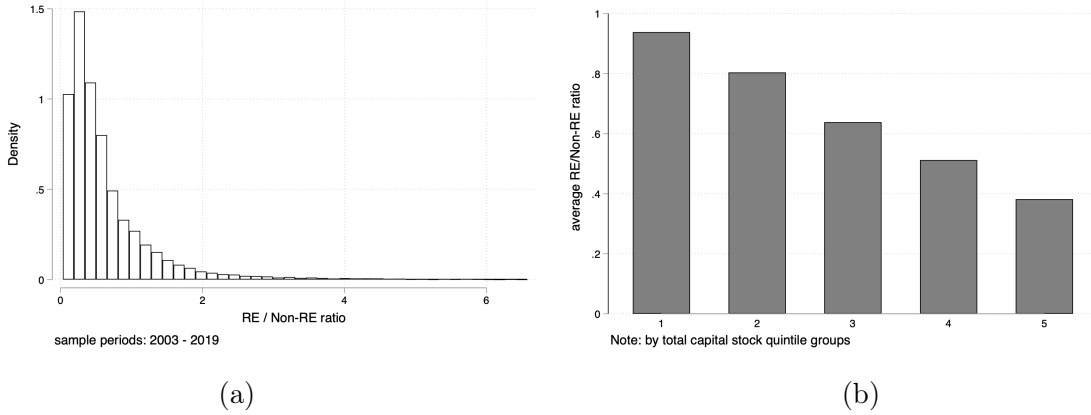


Figure 1: Distribution of RE/Non-RE ratio

Source: Financial Reports of Listed Companies in China. Based on asset types classified by the author.

4.2 Estimation Procedure

The SMM estimator minimises the distance between the data moments M and the simulated moments $\tilde{M}(\Theta)$ as in equation (7). For a given set of model parameters $[\gamma, F_k, \omega, F_h, \phi_k, \phi_h]$, I solve the capital adjustment model and simulate a stationary distribution of 3000 firms for 100 periods. I compute the simulated moments using the simulated data. $\tilde{M}(\Theta)$ is thus a function of Θ .

$$\hat{\Theta}_{smm} = \underset{\Theta}{argmin} (M - \tilde{M}(\Theta))' W (M - \tilde{M}(\Theta)) \quad (7)$$

W is the weighting matrix, obtained via bootstrap. I draw N_{sample} samples using block bootstrapping clustered at the firm level and compute the moments for each bootstrapped sample. The weighting matrix is given by the inverse of the matrix \hat{V} , which is computed as follows:

$$\hat{V} = \frac{1}{N_{\text{sample}}} \sum_{i=1}^{N_{\text{sample}}} (\text{moments}_{\text{sample},i} - \text{moments}_{\text{data}})' (\text{moments}_{\text{sample},i} - \text{moments}_{\text{data}}).$$

The algorithm for the multivariate global optimisation consists of two steps similar to Arnoud et al. (2019) and is described in detail in Appendix C.2. Appendix C.3 describes the procedure for obtaining the standard errors of parameter estimates.

4.2.1 Revenue Function Estimation

The revenue function parameters, including the curvature α , the share a , the elasticity of substitution σ , and the persistence parameter of the profitability process ρ_z are estimated by the generalised method of moments (GMM) with the moment conditions obtained from the quasi-differenced revenue function. Equation 8 is obtained by taking logs of the revenue function and quasi-differencing, where $K_{it} \equiv a^{\frac{1}{\sigma}} k^{\frac{\sigma-1}{\sigma}} + (1-a)^{\frac{1}{\sigma}} h^{\frac{\sigma-1}{\sigma}}$. The residual term ξ_{it} is the innovation to the profitability at t , which are orthogonal to k_{is} , h_{is} , and π_{is} , $\forall s \leq t-1$. Due to the time-to-build assumption for capital, ξ_{it} are also orthogonal to k_{it} and h_{it} , $\forall t$. The orthogonality conditions allow for the estimation of the four parameters α , a , σ , and ρ_z .

$$\log \pi_{it} = \rho_z \log \pi_{it-1} + \alpha \cdot (\log \mathbf{K}_{it} - \rho_z \log \mathbf{K}_{it-1}) + \xi_{it} \quad (8)$$

The GMM estimation proceeds as follows. I use the contemporaneous k_{it} , h_{it} and the lagged k_{it-1} , h_{it-1} , π_{it-1} as instruments. I also controlled for year dummies to remove the aggregate effect⁴. When σ converges to the limits 0, 1 or $+\infty$, the aggregation function converges to a Leontief, Cobb-Douglas or linear function, respectively. To avoid the non-smoothness and the numerical errors as the function converges to limits, and to exploit gradient information in the search for optima, I estimate the CES functional form and compare the cases where σ is fixed at different values from 0.05 to 2. The estimation follows the two-step procedure to obtain the efficiency.

Among all the scenarios, the specification with $\sigma = 0.05$ is the preferred one, suggesting that the aggregation between k and h are better approximated by a Leontief technology. First, the value of the objective function is smallest when σ is close to zero. Figure 2a plots the objective function of the GMM in both the first and second stages at different values of σ . The first stage uses an identity matrix as the weighting matrix, while the second stage uses a feasible optimal weighting matrix. In both stages, the objective function monotonically increases with σ . Second, the parameters are estimated more accurately when $\sigma = 0.05$.

⁴The year fixed effects (denoted as γ_t) are included as parameters to be estimated in the GMM, and the dummies are themselves instruments, since $\mathbb{E}(\gamma_t \xi_{it}) = 0$ holds for all t .

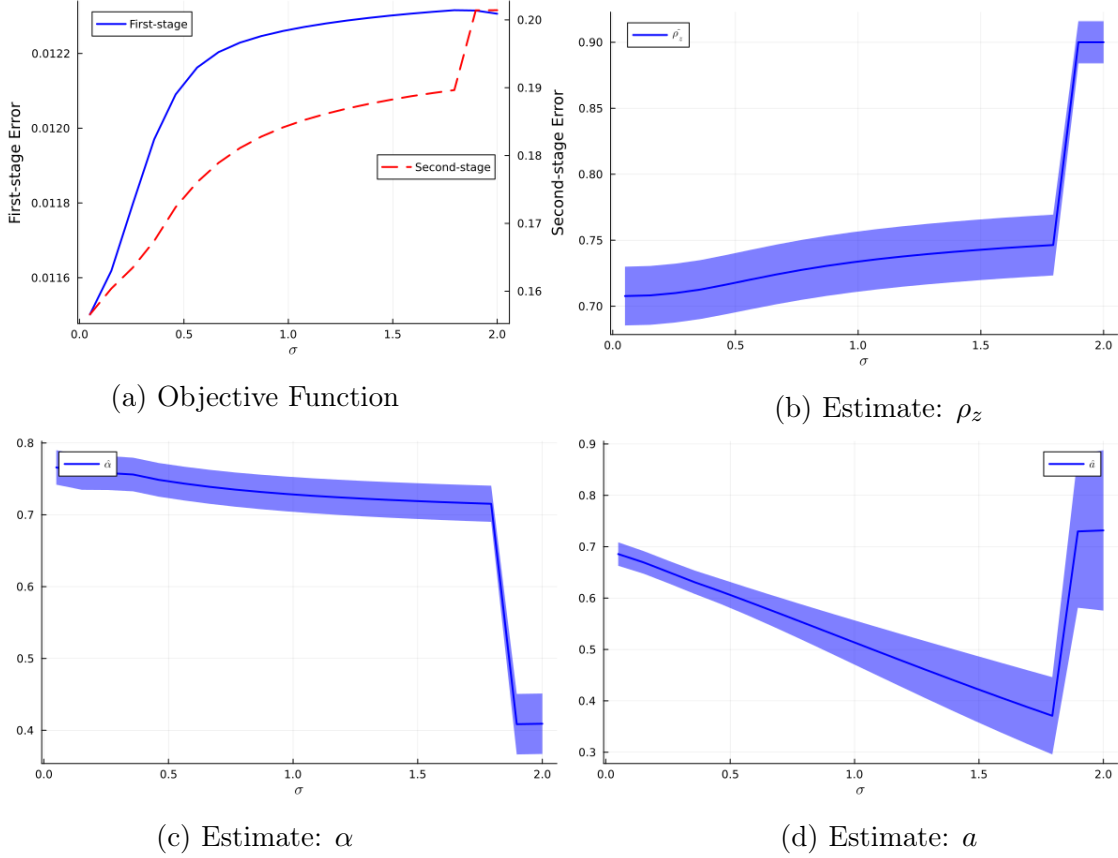


Figure 2: Revenue Function Estimation

Note: The GMM is performed to estimate ρ_z , α , and a while fixing σ at different values. Panel(a) displays the value of the objective functions obtained in the first and second stages. Panels (b), (c), (d) present the parameter estimates as functions of σ , with 95% confidence intervals included.

As shown in Figure 2 panels (b), (c), and (d), the parameter estimates exhibit significant jumps as σ increases, accompanied by a rise in standard errors. The estimates for $\hat{\rho}_z$ and $\hat{\alpha}$ remain fairly robust when σ is sufficiently small, whereas \hat{a} is estimated more accurately when $\sigma = 0.05$. To avoid the numerical errors due to the non-smoothness when the function is Leontief, I approximate the aggregator by a CES function with $\sigma = 0.05$ in the structural estimation. The simulation shows that the moments are very similar if the aggregation technology is instead a Leontief function.

The parameter estimates are summarised in table 2. Table A1 presents the complete estimation results. a is estimated at 0.6857. Together with the Leontief functional form, this share parameter a pins down the ratio between k and h in a frictionless economy, which is $\frac{1-\hat{a}}{\hat{a}} \approx 0.4584$. This is close to the sample median of the empirical distribution of the h/k ratio, which is about 0.4407.

After obtaining the estimates of α , a , σ , and ρ_z , I recover the idiosyncratic shocks \hat{z} by

plugging in the values of α , a and σ in the revenue function and removing the year fixed effects. I then estimate an AR(1) process with the residualized shocks to recover the variance of the innovation. The variance σ_z is estimated at 0.5716. Moreover, the persistence ρ_z in the AR(1) process estimation is similar to the estimates obtained from GMM.

The sample for the GMM estimation is an unbalanced panel. Since the entry and exit of firms in the sample are endogenous to profitability, this may bias the estimates. Incorporating entry and exit into the estimation is tricky since firms enter the sample when they go public and exit the sample when they delist, and modelling the listing process is beyond the scope of this paper. Instead of a structural approach, I use the same tools and procedures for GMM estimation on a strictly balanced panel. The results shown in table A2 indicate that the objective function is smallest when $\sigma = 0.05$, and the estimate of a is about 0.7. For the balanced panel, the persistence of the idiosyncratic shock process is higher, and the curvature of the return function is lower. This is consistent with the selection bias that may result from picking the “winners” after balancing the data.

4.2.2 Other Pre-defined Parameters

Table 2 describes the pre-defined parameters. The discount factor is set to 0.9479, corresponding to an interest rate of 5.5%. This is the weighted average of the one-year benchmark RMB loan rate during the sample period. The relative price of h is 1.5522 and is obtained by taking the sample average of the estimated relative price for all the firm-year observations. More details are described in the Appendix A.3. The depreciation rates for non-real-estate capital and real estate capital are set to 0.1275 and 0.0487, respectively, based on the sample averages of the in-use depreciation rates. They are also used in the construction of the capital stock.

Table 2: Model Parameters

	Value	Description	Source
β	0.9479	discount factor	$\frac{1}{1+r}$, $r = 0.055$
p	1.5522	relative price of h	sample mean
δ_k	0.1275	depreciation rate of k	in-use depreciation rate
δ_h	0.0487	depreciation rate of h	in-use depreciation rate
α	0.7659	curvature of revenue function	GMM estimation
σ	0.0500	CES elasticity of substitution	Leontief aggregator
a	0.6857	share of k	GMM estimation
ρ_z	0.7077	idiosync. prof.: persistency	GMM estimation
σ_z	0.5716	idiosync. prof.: stand. dev.	GMM estimation

4.2.3 Data Moments

The adjustment cost parameters and the pledgeability parameters of non-real-estate and real estate capital need to be estimated. The targeted data moments are summarised in table 3. The targeted moments include serial correlations of the investment rates of k and h , and the probability of investment spikes, defined as the probability of investment rates exceeding 30%⁵. The targeted moments also include the sample mean and median of the h/k (RE/Non-RE) ratio. These two moments indicate the proportion of real estate in the total capital stock and the skewness of the capital composition distribution. The calculation of the data moments is adjusted for year fixed effects⁶. All moments are calculated using the sample of the unbalanced panel. Only 514 firms are listed in all years of the sample period and have continuous information from 2003 to 2019, and balancing the panel may introduce a selection bias. Nevertheless, the data moments regarding investment rates are similar in the unbalanced and balanced panel.

Table 3: Targeted Data Moments

Value	Description	Definition
0.0508	serial correlation of i_k	$corr(i_k^l, i_k)$
0.0281	serial correlation of i_h	$corr(i_h^l, i_h)$
0.3527	positive spikes of i_k	$spike_k^+ \equiv Pr(i_k > 30\%)$
0.2166	positive spikes of i_h	$spike_h^+ \equiv Pr(i_h > 30\%)$
0.6549	sample average of h/k	$\overline{h/k}$
0.4407	sample median of h/k	$med(h/k)$

4.3 Estimation Results

Table 4 reports all estimated parameters and the corresponding simulated moments. In addition to the targeted moments, I also show moments that describe the shape of the h/k ratio distribution. The five moments $\overline{h/k}_{Q1} \dots \overline{h/k}_{Q5}$ represent the average h/k ratio for firms in each capital size quintile group. As shown in Figure 1 panel (b), the average h/k ratio decreases with capital size in the data. $skew(h/k)$ denotes the skewness of the h/k ratio distribution.

⁵There is a concern of using absolute spikes because the average investment rate of the sample is rather high, and a high investment rate in absolute terms (e.g. more than 20%) may not reflect the investment lumpiness. I follow Power (1998) and define the relative investment spikes as the probability of firms' investment rates exceeding largely their normal investment rate, i.e., more than 2.5 times their average investment rates over the sample period. I show the untargeted moments in appendix D.1

⁶I adjust the constructed variables by regressing them on year fixed effects, obtaining the residuals, and adding back the sample averages. This is to filter out the variations that are not due to idiosyncratic shock, and it leads to a lower serial correlation.

I compare the estimation results across different model specifications. Column (1) assumes $\phi_k = \phi_h = \infty$, indicating that the collateral constraints are never binding and there are no explicit financial frictions constraining external borrowing. Column (2) assumes $\phi_k = \phi_h = 0$ where the collateral constraints are most restrictive, and capital adjustments must be financed entirely through internal funding. The comparison of these two extreme scenarios provides insights into the model's mechanism. Column (3) assumes $\phi_k = \phi_h > 0$, and Column (4) further relaxes this restriction, allowing ϕ_k and ϕ_h to differ.

The comparison between the extreme cases in columns (1) and (2) demonstrates how financial frictions affect firm investment. In the presence of a strict financial constraint, investments are smoothed across periods, resulting in higher serial correlations and fewer investment spikes. The distribution of the h/k ratio is less skewed, and there is no clear correlation between capital size and asset composition. In contrast, the model without explicit financial frictions can generate a skewed h/k ratio distribution. The average h/k ratio is much higher than the median h/k ratio, with skewness close to the observed value. There is a downward trend in the h/k ratio as capital size increases, although not perfectly ordered, with $\overline{h/k}_{Q3}$ greater than $\overline{h/k}_{Q2}$ and $\overline{h/k}_{Q5}$ greater than $\overline{h/k}_{Q4}$. Overall, the model without explicit financial frictions fits the data moments better. This is further demonstrated by the estimation result in column (3), where the model allows assets to be pledgeable but restricts $\phi_k = \phi_h$. The pledgeability parameter is significantly different from zero, and the distance from the targeted moments is similar to that in column (1). In column (4), the estimation suggests that allowing different ϕ_k and ϕ_h further improves the model fit compared to the model assuming $\phi_k = \phi_h = +\infty$, as the distance is significantly smaller⁷. More importantly, the model generates a negative correlation between the h/k ratio and capital size, even though these are untargted in the estimation.

Across all the model specifications, the non-convex adjustment costs F_k and F_h are robustly estimated. The estimates suggest that adjustments to real estate capital involve a much higher fixed cost. Due to the complementarity between k and h , lumpy adjustments in h lead to lumpy adjustments in k . This results in a positive spike rate in k despite the small fixed cost parameter. F_h is estimated to be 0.2684 in the full-fledged model displayed in column (4), equivalent to 24% of flow revenue on average when there are positive investments in real estate capital. The high fixed cost of adjusting h compared to k helps to generate a non-degenerate distribution of the composition between k and h . Due to the high F_h , firms tend to adjust k while remaining inactive on the adjustment of h . The asset composition, therefore, varies across heterogeneous firms as they choose k' differently according to the realisation of the shock, conditional on the capital states k and h , even when they choose the same h' . The presence of high fixed costs of adjusting h also results in the highest h/k ratio for the smallest firms. This is because smaller firms have higher marginal returns to capital and are more likely to invest even when investments incur high fixed costs, conditional on

⁷The SMM estimation uses the optimal weighting matrix. Therefore, the distance measures follow χ^2 distributions. Since the model in column (1) is nested with the model in column (4), a χ^2 difference test can be performed to compare the models. The more complex model provides a significantly better fit with a p-value of 0.00064.

Table 4: Estimation Results

	(1) AC	(2) AC+FC(limit)	(3) AC+FC(sym.)	(4) AC+FC	Data
A. Model Parameters					
γ	0.0068 (0.0010)	0.0200 (0.0153)	0.0070 (0.0012)	0.0061 (0.0097)	
F_k	0.0015 (0.0015)	0.0021 (0.0006)	0.0013 (0.0005)	0.0029 (0.0048)	
ω	0.0992 (0.0278)	0.0144 (0.0094)	0.0419 (0.0087)	0.0233 (0.0925)	
F_h	0.2541 (0.0064)	0.3983 (0.0179)	0.3049 (0.0078)	0.2684 (0.0425)	
ϕ_k	$+\infty$	0	2.6737 (0.2053)	2.3283 (1.3100)	
ϕ_h	$+\infty$	0	2.6737 (0.2053)	2.5466 (0.3221)	
B. Moments					
$corr(i'_k, i_k)$	0.0080	0.0832	0.0180	0.0204	0.0508
$corr(i'_h, i_h)$	0.0293	0.0661	0.0502	0.0269	0.0281
$spike_k^+$	0.2393	0.1748	0.2441	0.2551	0.3527
$spike_h^+$	0.1420	0.0978	0.1406	0.1589	0.2166
$\overline{h/k}$	0.6951	0.5558	0.6826	0.6603	0.6549
$med(h/k)$	0.4822	0.4979	0.4754	0.4728	0.4407
$\overline{h/k}_{Q1}$	1.20	0.55	1.10	1.20	0.94
$\overline{h/k}_{Q2}$	0.65	0.56	0.65	0.62	0.80
$\overline{h/k}_{Q3}$	0.67	0.58	0.66	0.51	0.64
$\overline{h/k}_{Q4}$	0.47	0.58	0.47	0.48	0.51
$\overline{h/k}_{Q5}$	0.48	0.51	0.52	0.47	0.38
$skew(h/k)$	3.23	1.84	3.45	3.69	3.31
Distance	50.795	419.656	53.092	36.088	-

Note: The table presents the SMM estimation results for different model specifications, denoted as AC (adjustment costs) and AC+FC (adjustment costs and financial constraints). Panel A shows the model parameter estimates, with standard errors in parentheses, while Panel B displays the corresponding targeted and untargeted moments. The parameters in bold are estimated by targeting the moments in bold. The last column shows the data moments. “Distance” measures the discrepancy with respect to the targeted moments, as defined in equation 7.

the productivity realisation.

The convex adjustment costs vary across the model specifications. As explained in section 3, the convex costs smooth the investment process and account for the gradual adjustment due to limited financial capacity. This explains why the convex cost parameters take different values when the collateral constraints are specified differently. γ and ω are estimated to be higher in the economy without explicit collateral constraints, as in column (1), compared to the estimates in the economy with the most restrictive collateral constraints, as in column (2), though the difference is significant only for γ . Although the model estimated in column (1) doesn't explicitly model financial frictions, the convex costs can already account for the gradual adjustments induced by limited financial capacity. The model with two capital inputs and collateral constraints allows for identifying the different components in the quadratic costs: costs due to financial constraints and costs due to technological capabilities.

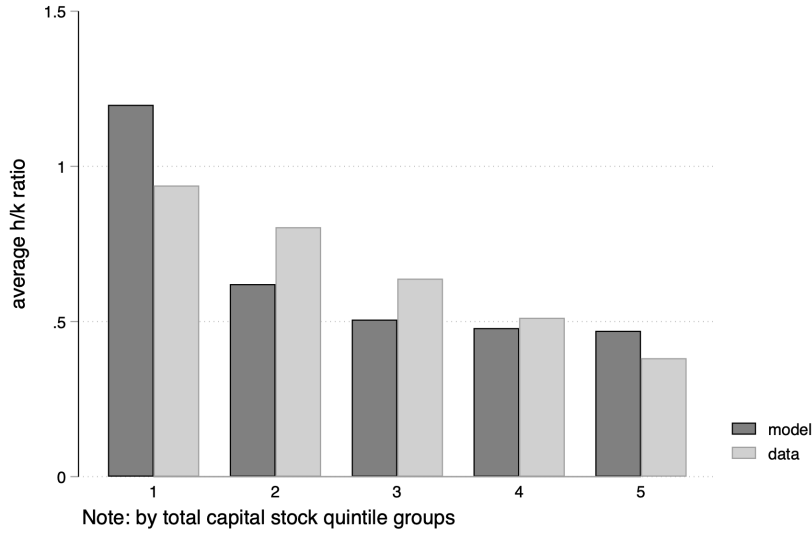
The pledgeability of k (h) is 2.3283 (2.5466), which implies that one unit of k (h) can secure external financing equivalent to 2.3283 (2.5466) units of k (h). These estimates are greater than 1 and are higher than the values typically used in the calibration of macroeconomic models. As discussed earlier in Section 3, the model abstracts from key financial decisions, which may explain these high estimates. While our analysis in Appendix A.4 shows that cash accumulation is not significantly observed before investment spikes, we do find evidence of intertemporal debt persisting for two years, which would make the collateral constraints less frequently binding. Moreover, firms may obtain external funding through unsecured loans or earnings-based borrowing that doesn't explicitly require collateral, though such financing could still be implicitly connected to a firm's capital holdings and overall creditworthiness. The high pledgeability estimates thus capture not only the liquidation value of assets, but also incorporate the lower frequency of binding constraints and the availability of alternative financing sources. Therefore, these estimates should not be interpreted as direct equivalents to observed liquidation ratios or haircuts in collateralised borrowing contracts, but rather as upper bounds that reflect the broader external funding capacity associated with holding specific types of capital assets.

4.4 Role of Collateral Constraints

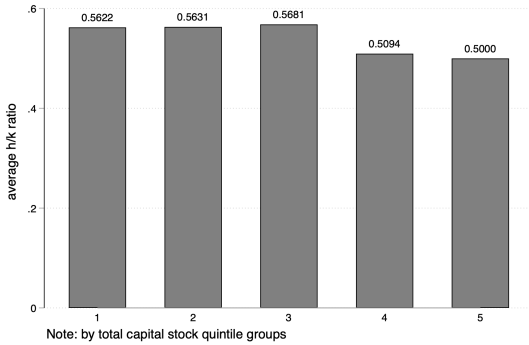
The occasional binding constraints and the asymmetry in the pledgeabilities of the capital assets k and h are essential in matching the observed feature of the h/k ratio, including the skewness and the negative correlation between the h/k ratio and capital size. As displayed in Table 4 column (1)-(3), the model that restricts pledgeability to be symmetric cannot account for the negative correlation between the h/k ratio and capital size.

Furthermore, Figure 3 compares the average h/k ratio for firms in capital size quintile groups in the simulated economies where γ , F_k , ω , and F_h are fixed at their estimates in the preferred model specification. Panel (a) compares the distribution generated in the preferred model specification to that in the data. Panels (b) and (c) plot the distribution in economies where

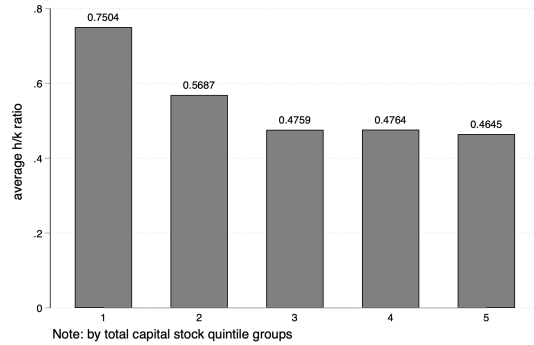
ϕ_k and ϕ_h are assumed to be symmetric and are set at either 0 (i.e., no external funding) or $+\infty$ (i.e., no constraints on external funding). These counterfactual economies alter both the slackness of the constraints and the asymmetry in pledgeability. As the collateral constraints become too tight, the correlation between capital size and asset composition becomes unclear, despite the asymmetry in the adjustment cost parameters. When the collateral constraints become too slack, there is a general trend of decline in the average h/k ratios. However, the average h/k ratios are similar in the last three quintile size groups. This is consistent with the moments displayed in Table 4, columns (1) and (3), and the mechanism is explained in Section 4.3.



(a) $\phi_k > 0, \phi_h > 0$



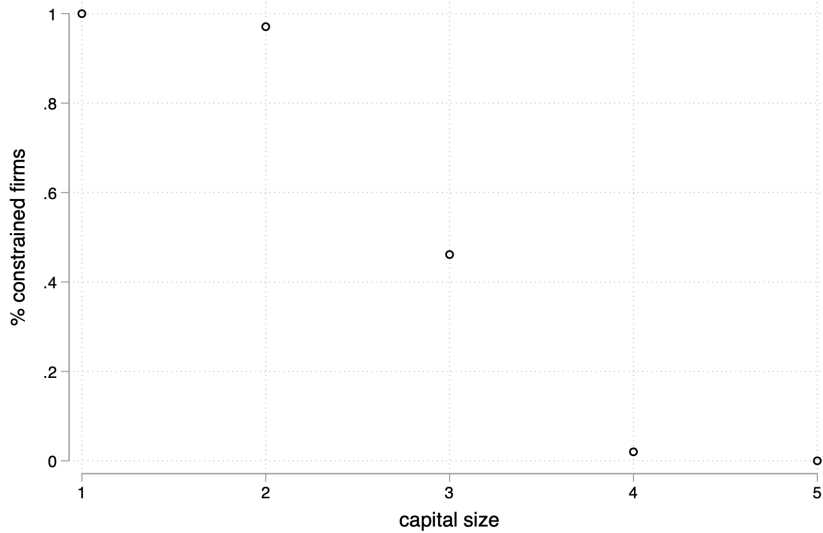
(b) $\phi_k = \phi_h = 0$



(c) $\phi_k = \phi_h = +\infty$

Figure 3: h/k ratio and Capital Size in Simulation

Note: In the simulation, γ, F_k, ω, F_h are the estimates as in Table 4 column (4). Total capital stock is defined as $k+h$. The observations are grouped into five bins according to the quintiles of total capital stock. The graph plots the average h/k ratio for each group.



Note: A firm is constrained if its constrained value is less than 97% of its unconstrained value.

Figure 4: Constrained firms and Capital Size

With collateral constraints and asymmetric pledgeability, as indicated by the precautionary saving motive, firms tend to tilt their investments towards more pledgeable assets if there are potentially binding constraints in the future. Figure 4 plots the share of constrained firms in capital size quintile groups in the preferred model simulation. A firm is constrained if the constrained value is less than 97% of its unconstrained value⁸. Figure 4 shows that smaller firms are more likely to be constrained, and as the capital size grows bigger, the share of constrained firms drops, and this coincides with the decreasing h/k ratio across size groups.

4.5 Identification of Parameters

Table 5 shows the elasticity matrices of the simulated moments with respect to the parameters in the model where $\phi_k = \phi_h = +\infty$ (AC) and where $\phi_k \neq \phi_h > 0$ (AC+FC). Each entry represents the elasticity of a simulated moment with respect to a model parameter in the neighbourhood of the parameter estimates. These elasticities also indicate which parameters are identified by which moments. The more sensitive a moment is to a parameter, the more informative that moment is in identifying the parameter. More details on the computation of the elasticity matrices are provided in Appendix C.3.

The comparison between the two elasticity matrices highlights the relationship between

⁸Instead of defining a firm as constrained if the current-period investments are at the corner, the difference in the values in the economies with and without constraints entails the effect of the potentially binding constraints in the future.

convex costs and financial constraints. The serial correlations are sensitive to γ and ω when there are no explicit financial constraints, but they become sensitive to ϕ_k and ϕ_h and less sensitive to γ and ω once financial constraints are introduced.

In both model specifications, the average h/k ratio is sensitive to changes in F_h , while the median h/k ratio is insensitive, given that the elasticity is approximated around a narrow neighbourhood of the parameter estimates. In the model with collateral constraints, the sample average and median h/k ratios are sensitive to F_h , ϕ_k , and ϕ_h , consistent with the model mechanisms discussed above.

Table 5: Elasticity of Moments to Parameters

a.Model AC						
Targeted Moments	Model Parameters					
	γ	F_k	ω	F_h		
$corr(i'_k, i_k)$	5.12	-2.09	13.38	-5.81		
$corr(i'_h, i_h)$	0.96	-0.77	2.92	3.04		
$spike_k^+$	0.02	-0.01	0.02	-0.09		
$spike_h^+$	0.01	-0.04	0.08	-1.14		
$\overline{h/k}$	-0.14	0.02	-0.06	0.45		
$med(h/k)$	-0.07	0.00	-0.02	0.05		
b. Model AC+FC						
Targeted Moments	Model Parameters					
	γ	F_k	ω	F_h	ϕ_k	ϕ_h
$corr(i'_k, i_k)$	2.70	2.08	1.92	13.04	19.63	6.66
$corr(i'_h, i_h)$	1.57	0.24	0.06	10.54	3.45	2.92
$spike_k^+$	-0.04	-0.04	-0.02	-0.44	0.04	-0.30
$spike_h^+$	-0.02	-0.04	0.03	-0.14	0.45	0.18
$\overline{h/k}$	-0.05	-0.03	-0.02	-0.29	-0.25	-0.27
$med(h/k)$	0.00	0.00	0.00	-0.15	-0.04	0.05

5 Counterfactual Exercises

5.1 Decomposition of the Effects of Frictions

In the model, the distribution of real estate and non-real-estate capital is determined by production technology, heterogeneous adjustment costs, and heterogeneous pledgeability. I decompose the effects of these channels by comparing three different economies in simulation: the baseline case with both collateral constraints and fixed adjustment costs, the case without

financial frictions but with fixed costs, and the case with neither financial frictions nor fixed costs. Table 6 shows the results.

The average h/k ratio is 0.656 in the baseline model. It decreases by 16% if there are no financial constraints and by 28% if there are neither financial frictions nor fixed adjustment costs. In the latter case, the average h/k ratio is close to the optimal composition implied by the Leontief aggregation technology. On the other hand, aggregate fixed assets (the sum of real estate and non-real-estate assets) decrease if there are no financial frictions and increase if there are no financial frictions and no fixed costs. The presence of financial frictions provides additional incentives to invest in collateralisable assets in the frictional economy, resulting in over-investment and distortion in the asset composition. Consistently, aggregate capital decreases by 4% and aggregate revenue decreases by 0.8% when there are no financial frictions. The removal of fixed costs brings the asset composition closer to the optimum and allows firms to grow larger. In this counterfactual economy, aggregate capital increases by 36.7% and aggregate revenue increases by 31.8%.

Meanwhile, aggregate TFPR (i.e., profitability weighted by capital size) increases as financial constraints and fixed adjustment costs are removed. The removal of financial frictions accounts for a 5% increase in aggregate profitability, as firms with positive profitability shocks can grow larger. Interestingly, when both financial constraints and fixed costs are removed, aggregate TFPR increases by only 3%, suggesting that high adjustment costs act as a filter that favours firms with higher profitability.

Table 6: Counterfactual Exercise

model	$\overline{h/k}$	$\overline{h/k}, \%$	agg. profitability	agg. revenue	agg. fixed assets
baseline	0.656		1	1	1
no FC	0.549	-16%	1.050	0.992	0.960
no FC & no AC	0.471	-28%	1.032	1.318	1.367
$\phi_h = 0$	0.596	-9%	0.964	0.997	1.030

5.2 Change in Real Estate Pledgeability

Table 6 illustrates the effects of a real estate crisis where real estate assets become non-pledgeable, offering an exploration of the consequences of the recent Chinese real estate crisis. While the crisis impacts firms' production from the demand side, it also limits their ability to pledge real estate assets as collateral due to declining and more volatile real estate prices. This introduces significant challenges from the supply side, particularly when firms rely on real estate collateral to fund investments. This counterfactual analysis underscores the critical role of real estate pledgeability in shaping firms' capital allocation decisions under collateral constraints and its broader implications for economic performance during periods of real estate crisis.

In the simulation, removing the collateral value of real estate assets (h) makes financial constraints more binding and increases the relative pledgeability of non-real-estate assets (k). This shift leads to a 9% decrease in the average h/k ratio, aligning the asset composition more closely with the theoretical optimum determined by production technology. Additionally, tighter constraints and higher collateral value lead to a 3% increase in aggregate capital. However, these improvements come at a cost: aggregate TFPR declines by 3.6%, and aggregate revenue decreases by 0.3%, highlighting the distortions caused by restricted access to external financing.

6 Conclusion

This paper investigates firms' asset composition and investment behaviour in the presence of collateral constraints. Empirically, there is a high proportion of real estate assets in capital stock for Chinese listed firms, and this share decreases with the size of the capital. By estimating a capital adjustment model with non-convex adjustment costs and collateral constraints, I find that the inclusion of financial frictions significantly enhances the model's explanatory power, particularly in accounting for observed asset composition distribution.

This paper provides a quantification of the effect of collateral constraints. Absent financial frictions, the proportion of real estate within the capital stock would decrease. Furthermore, it identifies distinct cost structures, including both convex and non-convex costs, associated with different asset types. The quantitative model in this paper provides a preliminary framework for studying the impact of real estate risk in the Chinese economy from the supply side through financial frictions.

However, certain limitations warrant consideration. The model's abstraction from dynamic debt decision means that the estimates of pledgeability are not directly interpretable as the observed collateral haircut. This also limits the identification since debt-related variables cannot be directly targeted in the estimation. Future research could extend the model with debt as a dynamic decision, thus providing a more realistic characterisation of firms' problems.

References

- Andrew B. Abel and Janice C. Eberly. A unified model of investment under uncertainty. *The American Economic Review*, 84(5):1369–1384, 1994. ISSN 0002-8282. URL <https://www.jstor.org/stable/2117777>.
- Andrew B. Abel and Janice C. Eberly. The effects of irreversibility and uncertainty on capital accumulation. *Journal of Monetary Economics*, 44(3):339–377, 1999. ISSN 0304-3932. doi: 10.1016/S0304-3932(99)00024-0.
- Philippe Aghion, George-Marios Angeletos, Abhijit Banerjee, and Kalina Manova. Volatility and growth: Credit constraints and the composition of investment. *Journal of Monetary Economics*, 57(3):246–265, April 2010. ISSN 0304-3932. doi: 10.1016/j.jmoneco.2010.02.005.
- Heitor Almeida, Murillo Campello, and Michael S. Weisbach. The cash flow sensitivity of cash. *The Journal of Finance*, 59(4):1777–1804, 2004. ISSN 0022-1082. doi: 10.1111/j.1540-6261.2004.00679.x.
- Antoine Arnoud, Fatih Guvenen, and Tatjana Kleineberg. Benchmarking Global Optimizers. Technical Report w26340, National Bureau of Economic Research, Cambridge, MA, October 2019.
- Saleem Bahaj, Angus Foulis, and Gabor Pinter. Home Values and Firm Behavior. *American Economic Review*, 110(7):2225–2270, July 2020. ISSN 0002-8282. doi: 10.1257/aer.20180649.
- Thomas W. Bates, Kathleen M. Kahle, and René M. Stulz. Why do us firms hold so much more cash than they used to? *The Journal of Finance*, 64(5):1985–2021, 2009. ISSN 0022-1082. doi: 10.1111/j.1540-6261.2009.01492.x.
- Loren Brandt, Johannes Van Biesebroeck, and Yifan Zhang. Creative accounting or creative destruction? Firm-level productivity growth in Chinese manufacturing. *Journal of Development Economics*, 97(2):339–351, March 2012. ISSN 03043878. doi: 10.1016/j.jdeveco.2011.02.002.
- Sylvain Catherine, Thomas Chaney, Zongbo Huang, David Sraer, and David Thesmar. Quantifying Reduced-Form Evidence on Collateral Constraints. *The Journal of Finance*, 77(4): 2143–2181, 2022. ISSN 1540-6261. doi: 10.1111/jofi.13158.
- Thomas Chaney, David Sraer, and David Thesmar. The Collateral Channel: How Real Estate Shocks Affect Corporate Investment. *American Economic Review*, 102(6):2381–2409, May 2012. ISSN 0002-8282. doi: 10.1257/aer.102.6.2381.
- Pu Chen, Chunyang Wang, and Yangyan Liu. Real estate prices and firm borrowings: Micro evidence from China. *China Economic Review*, 36:296–308, December 2015. ISSN 1043-951X. doi: 10.1016/j.chieco.2015.10.002.

- Andrea Chiavari and Sampreet Goraya. The Rise of Intangible Capital and the Macroeconomic Implications. page 79.
- Russell W Cooper and John C. Haltiwanger. On the Nature of Capital Adjustment Costs. *REVIEW OF ECONOMIC STUDIES*, page 23, 2006. doi: 10.1111/j.1467-937X.2006.00389.x.
- Mark Doms and Timothy Dunne. Capital Adjustment Patterns in Manufacturing Plants. *Review of Economic Dynamics*, 1(2):409–429, April 1998. ISSN 1094-2025. doi: 10.1006/redo.1998.0011.
- C. Fritz Foley, Jay C. Hartzell, Sheridan Titman, and Garry Twite. Why do firms hold so much cash? a tax-based explanation. *Journal of Financial Economics*, 86(3):579–607, 2007. ISSN 0304-405X. doi: 10.1016/j.jfineco.2006.11.006.
- Jie Gan. Collateral, debt capacity, and corporate investment: Evidence from a natural experiment. *Journal of Financial Economics*, 85(3):709–734, September 2007. ISSN 0304-405X. doi: 10.1016/j.jfineco.2006.06.007.
- Christoph Görtz, Plutarchos Sakellaris, and John D. Tsoukalas. Firms’ financing dynamics around lumpy capacity adjustments. *European Economic Review*, 156:104481, 2023. ISSN 0014-2921. doi: 10.1016/j.euroecorev.2023.104481.
- Fumio Hayashi. Tobin’s Marginal q and Average q: A Neoclassical Interpretation. *Econometrica*, 50(1):213–224, 1982. ISSN 0012-9682. doi: 10.2307/1912538.
- Hui Liang James and Roger Lirely. The propensity to save: The effect of sarbanes–oxley act. *Review of Financial Economics*, 40(1):77–96, 2022. ISSN 1058-3300. doi: 10.1002/rfe.1140.
- Amir Kermani and Yueran Ma. Asset Specificity of Nonfinancial Firms*. *The Quarterly Journal of Economics*, 138(1):205–264, February 2023. ISSN 0033-5533. doi: 10.1093/qje/qjac030.
- Nobuhiro Kiyotaki and John Moore. Credit Cycles. *Journal of Political Economy*, 105(2): 211–248, April 1997. ISSN 0022-3808. doi: 10.1086/262072.
- Kiminori Matsuyama. Credit Traps and Credit Cycles. *American Economic Review*, 97(1): 503–516, March 2007. ISSN 0002-8282. doi: 10.1257/aer.97.1.503.
- Virgiliu Midrigan and Daniel Yi Xu. Accounting for Plant-Level Misallocation.
- Virgiliu Midrigan and Daniel Yi Xu. Finance and Misallocation: Evidence from Plant-Level Data. *American Economic Review*, 104(2):422–458, February 2014. ISSN 0002-8282. doi: 10.1257/aer.104.2.422.
- Merton H. Miller and Daniel Orr. The demand for money by firms: Extensions of analytic results. *The Journal of Finance*, 23(5):735–759, 1968. ISSN 0022-1082. doi: 10.1111/j.1540-6261.1968.tb00353.x.

- Benjamin Moll. Productivity Losses from Financial Frictions: Can Self-Financing Undo Capital Misallocation? *American Economic Review*, 104(10):3186–3221, October 2014. ISSN 0002-8282. doi: 10.1257/aer.104.10.3186.
- Øivind Anti Nilsen and Fabio Schiantarelli. Zeros and Lumps in Investment: Empirical Evidence on Irreversibilities and Nonconvexities. *Review of Economics and Statistics*, 85(4):1021–1037, November 2003. ISSN 0034-6535, 1530-9142. doi: 10.1162/003465303772815907.
- Pablo Ottonello and Thomas Winberry. Investment, Innovation, and Financial Frictions.
- Ander Perez-Orive. Credit constraints, firms’ precautionary investment, and the business cycle. *Journal of Monetary Economics*, 78:112–131, April 2016. ISSN 0304-3932. doi: 10.1016/j.jmoneco.2016.01.006.
- Laura Power. The Missing Link: Technology, Investment, and Productivity. *Review of Economics and Statistics*, 80(2):300–313, May 1998. ISSN 0034-6535, 1530-9142. doi: 10.1162/003465398557393.
- Jing Wu, Joseph Gyourko, and Yongheng Deng. Real estate collateral value and investment: The case of China. *Journal of Urban Economics*, 86:43–53, March 2015. ISSN 00941190. doi: 10.1016/j.jue.2014.12.006.
- Ping Yan. An Investigation into Capital Misallocation. *China Economic Quarterly*, 11(2): 489–520, 2012. ISSN 2095-1086.

Appendix

A Data and Variables

A.1 Construction of Capital Stock

I construct the capital stock of both real estate and non-real estate assets by the perpetual inventory method. It follows the following procedure:

- I obtain the gross investment every year by the change in the reported gross value of fixed assets. The nominal amount of gross investment every year is deflated to the base-year price, set as the price in 1990, by the capital goods price index.
- To infer the initial capital stock k_0 , I assume a linear depreciation process and a depreciable life of 30 years for real estate and 15 years for non-real estate capital⁹, and then use the ratio of the accumulated depreciation over the original value to estimate the average age of capital assets and thus the "average" purchasing year of the assets. I also assume the purchasing year of the assets is no earlier than 1991 (or the price change before 1991 is negligible), and infer k_0 by deflating the reported book value of fixed assets in the purchasing year.
- I use the sample median of the in-use depreciation rate during the sample period, which is 0.1253 for non-real estate assets and 0.0476 for real estate assets. The estimated depreciation rate for the overall capital is 0.0833, and this is comparable to Yan (2012) and Brandt et al. (2012). Yan (2012) finds a median depreciation rate of 9.5% in a sample of above-scale Chinese manufacturing firms during 2005-2007, and she uses 10% as the depreciation rate in the construction of capital stock. Brandt et al. (2012) uses a depreciation rate of 9% in the construction of capital stock with a sample of above-scale manufacturing firms during 1998-2007.
- The capital stock is imputed by the capital accumulation process $k_{t+1} = k_t(1 - \delta) + i_t$.

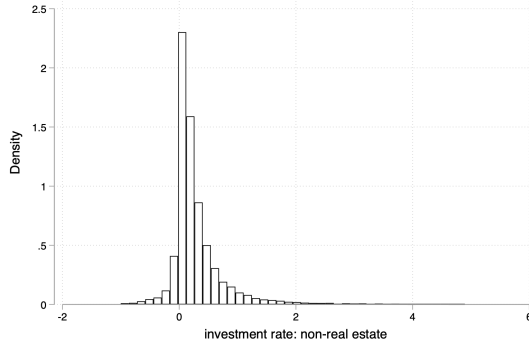
The book value of fixed assets may understate the capital inputs, as capital can be leased without being recorded as the firm's fixed assets. Information on leased capital is only available from 2021 onwards. For those firms that appear in the sample analysed in this paper, I compute the ratio of leased capital to net fixed assets for 2021 and 2022 and find that the distribution of the ratio is highly right-skewed, with 85% of the observations below 0.1.

⁹The depreciable life is estimated by (original value - salvage value) / annual depreciation for each firm-year observation by assuming zero salvage value. I take the sample median. This is comparable to Wu et al. (2015); they assume 25 years of depreciable life for buildings and 40 years of depreciable life for land.

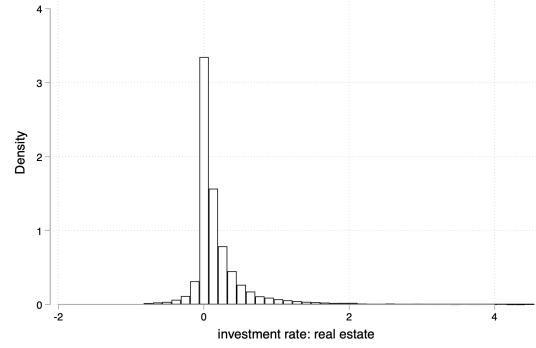
Another concern with the reported value of the real estate assets is that land cannot be privately owned, and part of the land-use rights are granted by the government to firms without charging the land transfer fees, in which case the land is classified as intangible assets and reported at fair value. I only include land classified as fixed assets as real estate capital primarily for two reasons: firstly, detailed classification information on intangible assets is only available after 2007 with a lot of missing values, which poses a significant challenge to correct measurement; secondly, the land-use right granted without fees¹⁰ doesn't involve investment payment, nor can they be used as collateral. Including these assets in real estate capital would introduce further measurement error since the model accounts for costly real estate investments and pledgeable assets. As a robustness check, I also compare the data moments computed using the original sample and the sample that takes into account land in intangibles and find that though the distribution of h/k ratio is shifted to the right due to the addition of land, the other targeted data moments remain similar, and the negative correlation between capital size and h/k ratio remains the same.

A.2 Description of Investment Rates

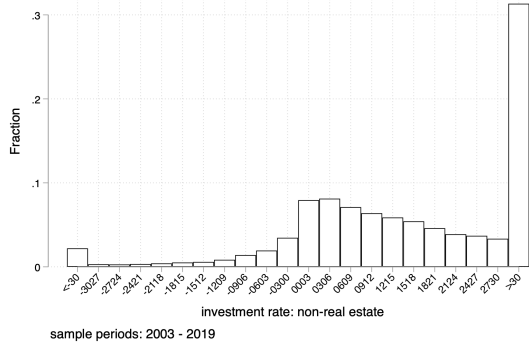
¹⁰ 划拨用地.



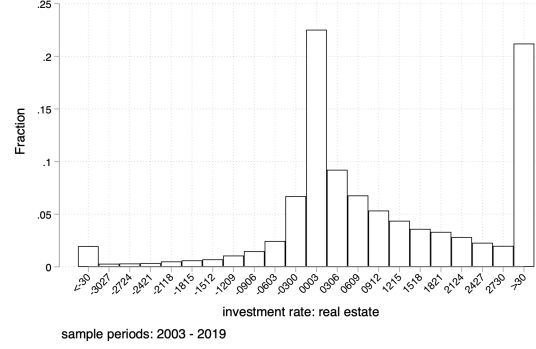
(a) non-real estate capital



(b) real estate capital



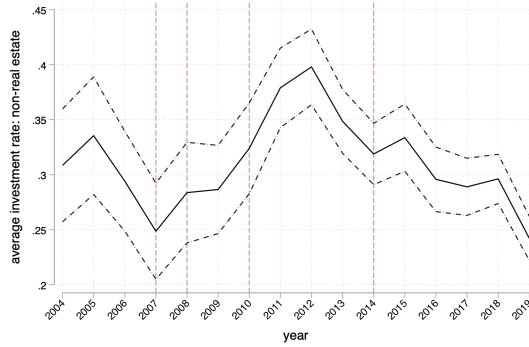
(c) non-real estate capital



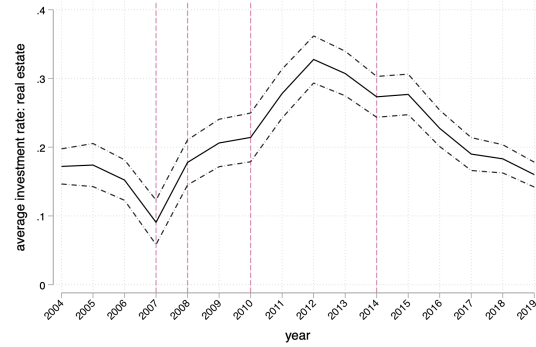
(d) real estate capital

Figure A1: Distribution of Investment Rates

Source: Financial Reports of Listed Companies in China. Based on asset types classified by the author.



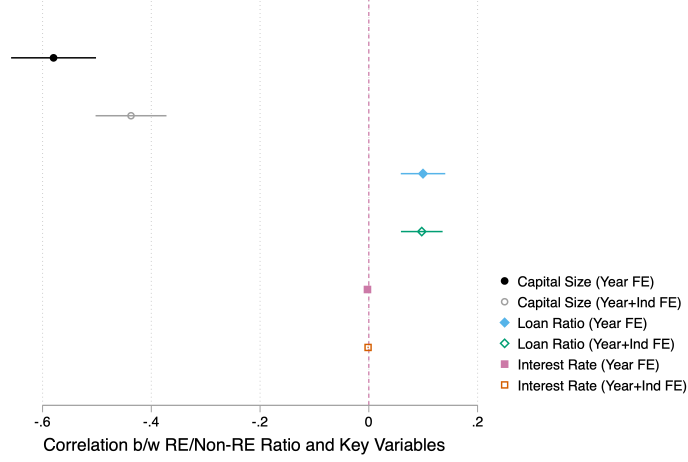
(a) non-real estate capital



(b) real estate capital

Figure A2: Trend of Investment Rates

Source: Financial Reports of Listed Companies in China. Based on asset types classified by the author.



Note: This graph displays estimated coefficients for the relationship between RE/Non-RE ratio and key variables in Chinese listed manufacturing firms (2003-2019). RE/Non-RE ratio represents the ratio of real estate to non-real estate capital stock constructed using the perpetual inventory method. Size measure is $\log(\text{RE} + \text{Non-RE capital})$, debt ratio is $(\text{short-term} + \text{long-term loans})/\text{net fixed assets}$, and interest rate is $\text{financial expenses}/\text{total debt}$. All relationships are estimated with standard errors clustered at the firm level, controlling for firm size (\log total capital) when measuring the debt ratio or interest rate. Two specifications are shown for each outcome: with year fixed effects only (filled markers) and with both year and industry fixed effects (hollow markers). Confidence intervals are at the 95% level. Source: Financial Reports of Listed Companies in China. Based on asset types classified by the author.

A.3 Relative Price of Real Estate Capital

Empirically, I obtain the relative price of real estate capital p in the following way:

- For each firm-year observation, I compute the ratio of nominal value (sum of past purchases - depreciation) to the real value of real estate capital (constructed by PIM). This can be considered as a weighted average of real estate capital purchase prices (in the past years before time t) weighted by the amount of real estate capital for each firm.
- I normalise the prices from the previous step by the price of non-real estate capital so that the prices are relative to the price of k . The 1% and 99% percentiles of the obtained prices are 0.78 and 4.62. The median is 1.56, and the mean is 1.76.

p is set as the sample mean of these prices. As a comparison, the relative price of buildings and structures to machines from the Price Index of Capital Goods ranges from 1.03 to 3.03 from 1990 to 2019. The mean and median of this relative price series are 1.93 and 1.896, respectively.

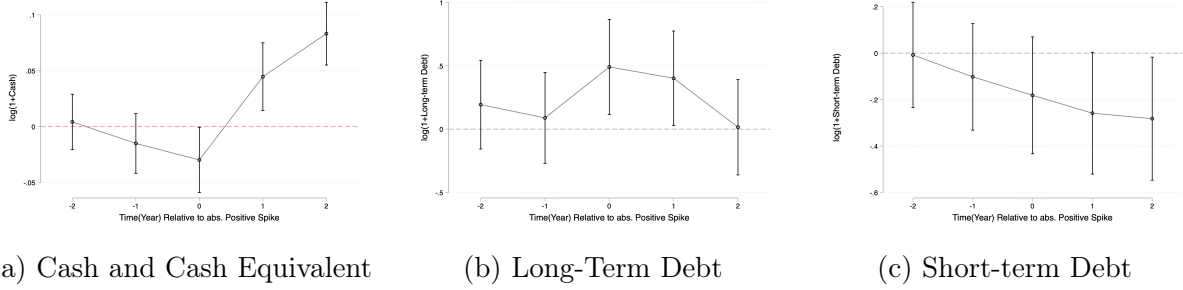


Figure A3: Cash/Debt Dynamics around Positive Investment Spikes

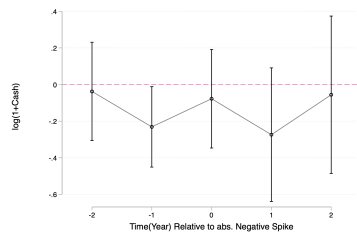
A.4 Cash/Debt and Investment Spikes

Görtz et al. (2023) shows that there is a build-up of cash stock before (anticipated) positive investment spikes. The cash stock drops during the lumpy adjustment period and recovers afterwards. This indicates that investments are primarily financed through internal funding. Following this reasoning, I test the dynamics of cash and debt around investment spikes by running the following regression:

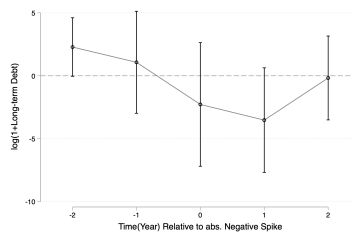
$$d_{it} = \sum_{h=-2}^2 \beta_h \times 1\{spike_{i,t+h}\} + \delta_t + \mu_i + x_{it} + \varepsilon_{it},$$

where the left-hand side variable d_{it} is the logged book value of cash, defined as cash and liquid financial assets, short-term debt, or long-term debt. Investment spikes are defined as absolute spikes when investment rates are greater than 0.3 or smaller than -0.3. Note that investment spikes can last for more than one period. The sample median and mean duration of positive investment spikes are 2 and 2.76 periods, respectively. β_h measures the average value of d two periods before and after the spike events, after removing the year and firm fixed effects and controlling for x (size and ownership structure).

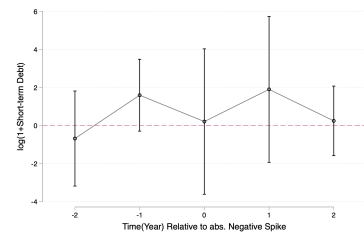
Figure A3 shows the cash and debt dynamics around positive investment spikes. Panel (a) indicates that there is no significant cash build-up before the investment spikes. There is a slight decrease in cash during the lumpy adjustment and an increase in cash after the spike. Panels (b) and (c) show that there is no significant change in short-term debt (due in less than one year), but a significant increase in long-term debt during the spike and one year after, followed by a significant drop two years after the spike. These results suggest that lumpy investments are financed more through debt rather than cash, and that the debt is repaid relatively quickly (within two years). Figure A4 shows no significant fluctuations in cash and debt around negative investment spikes. I also perform the test for relative investment spikes, and the results are similar.



(a) Cash and Cash Equivalent



(b) Long-Term Debt



(c) Short-term Debt

Figure A4: Cash/Debt Dynamics around Negative Investment Spikes

B Revenue Function Estimation

Table A1: Quasi-differenced Revenue Function Estimation

	$\hat{\rho}_z$	$\hat{\alpha}$	\hat{a}	$Dist$
$\sigma = 0.05$	0.7077 (0.011)	0.7659 (0.012)	0.6857 (0.012)	0.1566
$\sigma = 0.1526$	0.7082 (0.011)	0.7587 (0.012)	0.6694 (0.011)	0.1604
$\sigma = 0.2553$	0.7100 (0.011)	0.7581 (0.012)	0.6501 (0.011)	0.1635
$\sigma = 0.3579$	0.7127 (0.011)	0.7561 (0.012)	0.6307 (0.012)	0.1674
$\sigma = 0.4605$	0.7163 (0.011)	0.7487 (0.012)	0.6132 (0.012)	0.1724
$\sigma = 0.5632$	0.7203 (0.011)	0.7434 (0.012)	0.5947 (0.014)	0.1761
$\sigma = 0.6658$	0.7241 (0.012)	0.7389 (0.012)	0.5759 (0.015)	0.1789
$\sigma = 0.7684$	0.7275 (0.012)	0.7350 (0.012)	0.5569 (0.017)	0.1811
$\sigma = 0.8711$	0.7306 (0.012)	0.7318 (0.012)	0.5377 (0.019)	0.1828
$\sigma = 0.9737$	0.7332 (0.012)	0.7289 (0.012)	0.5184 (0.021)	0.1841
$\sigma = 1.0763$	0.7356 (0.012)	0.7265 (0.012)	0.4992 (0.024)	0.1852
$\sigma = 1.1789$	0.7377 (0.012)	0.7244 (0.012)	0.4802 (0.026)	0.1861
$\sigma = 1.2816$	0.7395 (0.012)	0.7225 (0.013)	0.4613 (0.028)	0.1869
$\sigma = 1.3842$	0.7411 (0.012)	0.7208 (0.013)	0.4426 (0.030)	0.1876
$\sigma = 1.4868$	0.7426 (0.012)	0.7192 (0.013)	0.4241 (0.033)	0.1882
$\sigma = 1.5895$	0.7440 (0.012)	0.7178 (0.013)	0.4061 (0.035)	0.1888
$\sigma = 1.6921$	0.7452 (0.012)	0.7165 (0.013)	0.3883 (0.037)	0.1892
$\sigma = 1.7947$	0.7464 (0.012)	0.7153 (0.013)	0.3709 (0.038)	0.1897
$\sigma = 1.8974$	0.9000 (0.008)	0.4085 (0.021)	0.7298 (0.076)	0.2014
$\sigma = 2$	0.9000 (0.008)	0.4092 (0.021)	0.7318 (0.080)	0.2014

Table A2: Quasi-differenced Revenue Function Estimation: Balanced Panel

	$\hat{\rho}_z$	$\hat{\alpha}$	\hat{a}	$\hat{\sigma}$	$Dist$
$\sigma = 0.05$	0.8469 (0.015)	0.6497 (0.032)	0.7255 (0.026)	n.a.	83.55
$\sigma = 0.5375$	0.8495 (0.015)	0.6352 (0.031)	0.6471 (0.030)	n.a.	87.22
$\sigma = 1.0250$	0.8497 (0.015)	0.6350 (0.031)	0.5744 (0.052)	n.a.	87.16
$\sigma = 1.5125$	0.8502 (0.015)	0.6342 (0.031)	0.5082 (0.079)	n.a.	86.96
$\sigma = 2.00$	0.8505 (0.015)	0.6335 (0.031)	0.4448 (0.105)	n.a.	86.86

Note: The estimates are obtained with a two-step GMM estimator. The sample is a balanced panel with 785 firms and 5 years (2015-2019).

C Simulated Method of Moments

C.1 Model Solution

The model is solved by value function iteration. There are dynamic choices, on both extensive and intensive margins, of two capital inputs. The value function iteration follows the following steps:

1. z is discretised with the Tauchen method on a coarse grid, denoted as zz . k and h are discretized on coarse grids (kk, hh) and fine grids $(\widetilde{kk}, \widetilde{hh})$.
2. The discretized value function V defined in equation 2 is on $(zz, \widetilde{kk}, \widetilde{hh})$. The discretized value function V^a, V^k, V^h, V^n defined in equation 3, 4, 5, and 6 are on (zz, kk, hh) . \widetilde{kk} are such that for any $k \in kk$, $k(1 - \delta_k) \in \widetilde{kk}$. The same applies to \widetilde{hh} .
3. For a guess $V_i(zz, \widetilde{kk}, \widetilde{hh})$:
 - For each $V_{i+1}^a, V_{i+1}^k, V_{i+1}^h, V_{i+1}^n$, find the optimal $(k, h) \in (\widetilde{kk}, \widetilde{hh})$ that maximizes the right hand side for every (z, k, h) state and update the values on the intensive margin.
 - Evaluate $V_{i+1}^a, V_{i+1}^k, V_{i+1}^h, V_{i+1}^n$ on the fine grid $(zz, \widetilde{kk}, \widetilde{hh})$, find the maximum among the four cases, and update the value and policy on the extensive margin. This gives $V_{i+1}(zz, \widetilde{kk}, \widetilde{hh})$
4. Given the converged V and V^a, V^k, V^h, V^n :

- Construct new grids that are finer for (z, k, h) , denoted as $(\widehat{z}\widehat{z}, \widehat{k}\widehat{k}, \widehat{h}\widehat{h})$. $\widehat{k}\widehat{k}$ are such that for any $k \in \widehat{k}\widehat{k}$, $k(1 - \delta_k) \in \widehat{k}\widehat{k}$. The same applies to $\widehat{h}\widehat{h}$.
- Interpolate V on $(\widehat{z}\widehat{z}, \widehat{k}\widehat{k}, \widehat{h}\widehat{h})$. For each state $(z, k, h) \in (\widehat{z}\widehat{z}, \widehat{k}\widehat{k}, \widehat{h}\widehat{h})$, find the policies on the extensive margin and intensive margin. This is to allow for simulation on the discretised state space. The simulation on the fine $\widehat{z}\widehat{z}$ ensures the variation in z , and the simulation on $\widehat{k}\widehat{k}, \widehat{h}\widehat{h}$ avoids the errors from interpolating around the kinks.

C.2 Optimization Algorithm

The algorithm is designed to find the global optimum by combining quasi-random initial sampling with iterative local optimisation. It consists of two main stages: the initial guess generation and the global optimisation search.

1. Initial Guess Generation

The algorithm begins by generating initial guesses for the parameters θ using a Halton sequence, which is a low-discrepancy, quasi-random sequence. This sequence is ideal for sampling because it covers the parameter space uniformly, reducing the risk of missing important regions.

- Parameter Space Definition:** Let θ be a vector of d parameters, each with bounds $\theta_i \in [l_i, u_i]$ for $i = 1, 2, \dots, d$.
- Halton Sequence Sampling:** The algorithm generates N points $\theta^{(1)}, \theta^{(2)}, \dots, \theta^{(N)}$ using the Halton sequence, ensuring that these points are uniformly distributed across the parameter space. Each point $\theta^{(i)}$ is scaled to respect the bounds $[l_i, u_i]$.
- Targeted Perturbation:** For a subset of parameters $\theta_{\text{perturb}} \subset \theta$, the algorithm optionally adds normally distributed perturbations to create a denser sampling in key areas. This generates additional points near each $\theta^{(i)}$, enhancing the sampling density in critical regions.

2. Global Optimisation Search

- Setup and Initialisation:** The search begins by initialising storage for local optima and setting up the bounds l_i and u_i for each parameter.
- Iterative Local Search:** The algorithm iteratively refines its search for the global minimum by:
 - Initial Guess Selection:** For each iteration i , the starting point $\theta^{(i)}$ is selected from the set of best initial guesses generated by the Halton sequence.

In the first iteration, $\theta^{(1)}$ is directly taken from the Halton points. For subsequent iterations, $\theta^{(i)}$ is computed as a weighted combination:

$$\theta^{(i)} = (1 - w_i)\theta_{\text{halton}}^{(i)} + w_i\theta_{\text{local}}^{(i-1)},$$

where $\theta_{\text{halton}}^{(i)}$ is the next Halton point, $\theta_{\text{local}}^{(i-1)}$ is the best local minimum from previous iterations, and w_i is a weight that increases with each iteration.

- ii. **Local Optimization:** The Nelder-Mead Subplex algorithm is applied starting from $\theta^{(i)}$ to find a local minimum $\theta_{\text{local}}^{(i)}$ and its corresponding objective function value $J(\theta_{\text{local}}^{(i)})$. This local minimum is then saved.
- (c) **Convergence Check:** The algorithm checks for convergence by evaluating the difference ϵ between consecutive local minima:

$$\epsilon = \|\theta_{\text{local}}^{(i)} - \theta_{\text{local}}^{(i-1)}\|_{\infty},$$

where $\|\cdot\|_{\infty}$ denotes the maximum norm. If $\epsilon \leq \text{tol}$, the algorithm converges; otherwise, it continues to the next iteration. The process also stops if the maximum number of iterations N^* is reached.

- (d) **Result Compilation:** After the iterations, the algorithm identifies the global minimum θ^* by selecting the parameter set with the lowest objective function value $J(\theta^*)$ from all local minima found. This global minimum is then saved and returned.

C.3 Standard Errors and Elasticity Matrix

This section outlines the methodology used to compute the standard errors of parameter estimates and the elasticity matrix as part of the post-estimation analysis. The process leverages local polynomial regression to approximate gradients and derive the Jacobian matrix.

1. Simulate moments around the parameter estimates: To calculate how the moments change with respect to the parameters, I generate a set of perturbed parameter values around the estimate \hat{x} . These values form a symmetric neighbourhood around \hat{x} . I simulate the corresponding moments for each $x_i \in x_{\text{vec}}$.
2. Local polynomial regression to compute derivatives: I approximate the gradient of the simulated moments with respect to the parameters using local polynomial regression. Given perturbed values x_{vec} and corresponding moment values m_{vec} , I fit a polynomial of degree $p = 3$.
3. Compute the gradients and the elasticities for each parameter x : For a model with k moments and n parameters, the Jacobian matrix J is a $k \times n$ matrix, where each element J_{ij} is

$$J_{ij} = \frac{\partial m_i}{\partial x_j},$$

and the entry of the elasticity matrix E is given by

$$E_{ij} = \frac{\partial m_i}{\partial x_j} \cdot \frac{\hat{x}_i}{m_j(\hat{x}_i)} = J_{ij} \cdot \frac{\hat{x}_j}{m_i(\hat{x}_j)}$$

4. Compute the standard errors: The variance-covariance matrix of the parameter estimates is

$$\text{VCV}_\theta = (J'WJ)^{-1}$$

Where:

- J is the Jacobian matrix,
- W is the weighting matrix, which is the inverse of the variance-covariance matrix of the data moments.

The standard errors of the parameter estimates are the square roots of the diagonal elements of the variance-covariance matrix:

$$\text{SE}(\theta_j) = \sqrt{(\text{VCV}_\theta)_{jj}}$$

D Additional Estimation Results

D.1 Untargeted Moments

Table A3: Untargeted Moments: Relative Investment Spikes

	(1)	(2)	(3)	(4)	Data
	AC	AC+FC(limit)	AC+FC(sym.)	AC+FC	
Untargeted Moments					
<i>rel.spike_k⁺</i>	0.18	0.13	0.19	0.19	0.11
<i>rel.spike_h⁺</i>	0.14	0.10	0.14	0.16	0.14
<i>rel.spike_k⁻</i>	0.00	0.00	0.00	0.00	0.01
<i>rel.spike_h⁻</i>	0.04	0.00	0.04	0.04	0.02